JOC The Journal of Organic Chemistry

pubs.acs.org/joc Article

Accounting for Strong Ligand Sensitivity in Pd-Catalyzed α-Arylation of Enolates from Ketones, Esters, and Nitroalkanes

Sergei Tcyrulnikov and Marisa C. Kozlowski*

Cite This: J. Org. Chem. 2020, 85, 3465−3472 Read Online

ACCESS | Metrics & More | Article Recommendations | Supporting Information

ABSTRACT: The mechanism of the Pd-catalyzed α-arylation of three model enolates is studied focusing on an analysis of their very different reactivities. In particular, the low reactivity of nitronates under standard arylation conditions and their high sensitivity to the nature of catalytic systems are addressed. The three canonical steps for each of the reaction systems are examined, and key trends surrounding the stability of intermediates and transition states are delineated. A framework based on molecular orbital analyses and the hard−soft acid−base (HSAB) theory is advanced to explain the observed reactivity trends. The local softness of the enolates was found to be a key parameter controlling the energy of the enolate−catalyst complexes. The low reactivity of the nitroalkane enolates is attributed to slow reductive elimination, a consequence of the hard nature of the nitronate. Analysis of reactivity of nitromethane in α-arylation with Pd catalysts containing Buchwald ligands reveals destabilization of the L_2Pd species as a major non-enolate-specific acceleration mechanism as well as less electron-rich ligands accelerating reductive elimination as a nitronate-specific mechanism. The corresponding energetics and feasibility that favor C-arylation versus O-arylation are outlined.

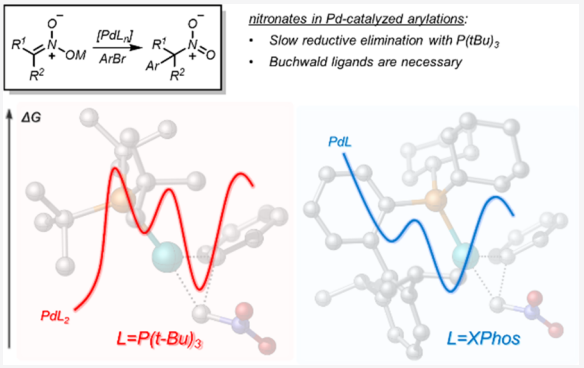

INTRODUCTION

The Pd-catalyzed α-arylation of enolates is a widely used and valuable reaction.[1] Intensive development of this reaction since the late 1990s quickly made this transformation a popular C−C bond formation method. The reaction is well studied for enolates derived from aldehydes, ketones, esters, malonates, amides, and nitriles.[2] Most of these enolates exhibit similar reactivity and some general conditions can be identified. Thus, the majority of arylation reactions (Scheme 1A) can be performed by combining appropriate bases (depending on the pK_a of the substrate, amide and carbonate bases are normally used), BINAP or P(*t*-Bu)$_3$ as a ligand, and aprotic low-polarity solvents (THF, dioxane, and toluene are typical).[3] Reports by Vogl and Buchwald and Muratake and Nakai[4] and our own studies[5] summarize approaches for arylation of various nitro compounds, allowing a range of substituted structures to be accessed (Scheme 1B).[6] Interestingly, nitro compounds are completely unreactive under general arylation conditions. Moreover, the transformation exhibits a very tight window of reactivity with respect to the structure of the ligand. These observations prompted our interest in understanding the mechanism of this reaction.

Quite surprisingly, despite a great number of synthetic papers published on the topic, only a few mechanistic studies have been performed,[7] and to the best of our knowledge, no computational studies have been reported. To gain more insight into the peculiarities of the reaction and the effects that the nature of the anion has on the efficiency and selectivity of transformation, we initiated a computational study of the mechanism. In this study, calculations of the nitronates are compared to those of enolates derived from ketones and esters to establish the driving forces behind their highly disparate reactivities. Specifically, the anions of acetone, methyl acetate, and nitromethane are examined. For the comparative analysis of the reactivity of enolates, P(*t*-Bu)$_3$ is used as a ligand. To further understand the reactivity of nitro compounds in the reaction, the performance of the XPhos versus *t*-Bu-XPhos catalytic systems is also analyzed.

RESULTS AND DISCUSSION

Oxidative Addition. The first step in the mechanism of these reactions is oxidative addition, and establishing the structure of the active catalyst is essential to modeling this step. The starting Pd(0) species can exist as mono- or polyligated species. In general, the equilibrium favors the more electronically saturated complexes (14, 16, or 18 electrons) if the ligand is not sterically hindered. However, such highly coordinated Pd

Received: November 27, 2019
Published: January 29, 2020

https://dx.doi.org/10.1021/acs.joc.9b03203
J. Org. Chem. 2020, 85, 3465−3472

Scheme 1. Typical Reaction Conditions for Arylation of Ketones and Esters and Examples of Conditions for Arylation of Different Types of Nitro Compounds

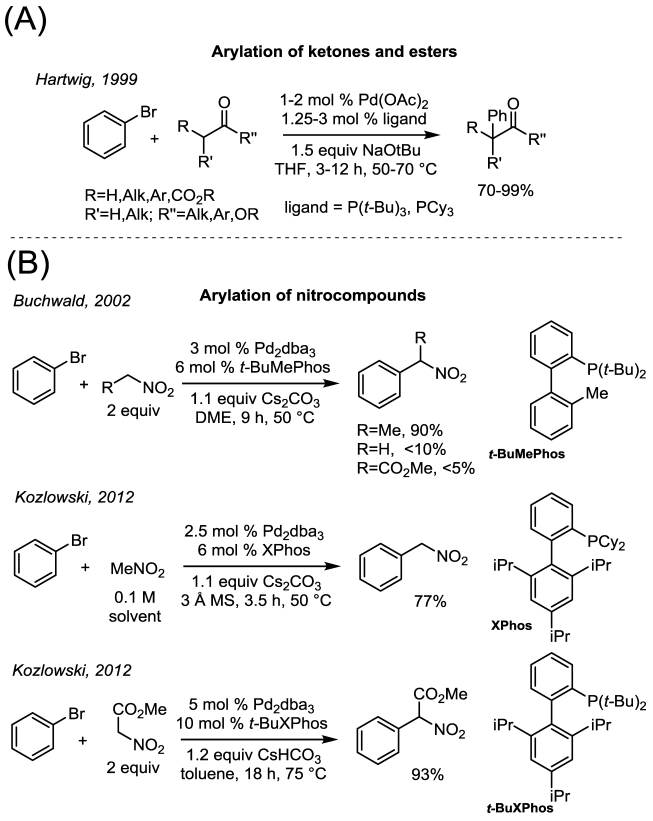

species exhibit poor reactivity in many common cross-coupling reactions, which require the formation of monoligated Pd. Thus, the reactivity in such systems is greatly improved when the ligand shifts the equilibrium toward the monoligated Pd.[8] Consistent with these ideas, calculations indicate that the oxidative addition is much faster starting from the L_1Pd species than the L_2Pd species (see Figure 1). Thus, for trimethyl phosphine, the L_1Pd complex was calculated to be ~80 times more reactive in oxidative addition than the corresponding L_2Pd complex. For bulky trialkyl phosphines, this situation is even more pronounced with the L_2Pd being virtually unreactive due to the severe steric interactions between ligands in the corresponding oxidative addition transition state. Therefore, ligand dissociation is an extremely important factor contributing to the rate of the process in question.

Oxidative addition places the aryl group trans to the bulky ligand, resulting in formation of the T-shaped isomer **iso3** (Figure 1). Due to the lack of an empty coordination site adjacent to the halogen, this isomer is not reactive in transmetallation and needs to first undergo isomerization. Two T-shaped adducts can undergo transmetallation, with **iso2** undergoing a low barrier transformation to afford the most stable **iso1**.

Transmetallation. Both isomers **iso1** and **iso2** can be attacked by the incoming enolate nucleophile. Our calculations of the model ketone system (sodium enolate of acetone, L = PMe_3) indicate that C attack of the enolate on both isomers is likely to proceed as a barrierless process (Figure 2, top). The energy of the system steadily decreases as the Pd−C distance decreases from 4 Å to the corresponding equilibrium value. It

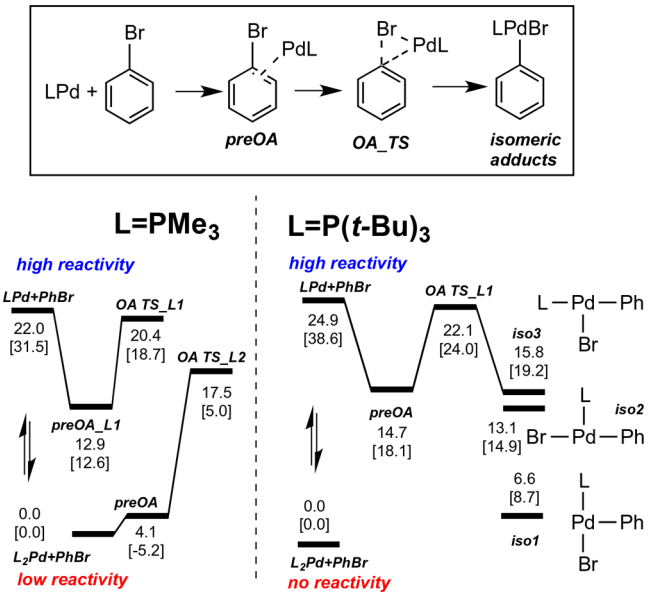

Figure 1. Oxidative addition of PhBr to trimethyl phosphine and tris-*tert*-butyl phosphine-ligated Pd. Free energies and enthalpies (in brackets) are in kcal/mol. Here and further, unless specified otherwise, the values are computed using rM06/6-311+G(d,p), Pd, Br: LANL2DZ, SMD: toluene // rB3LYP/6-31G(d), Pd, Br:LANL2DZ.

is unlikely that an early transition state with a Pd−C distance greater than 4 Å occurs given the corresponding Pd−C distances in the transmetallation product (2.34 Å), the oxidative addition complex (1.98 Å), and in the oxidative addition transition state (2.02 Å). In a similar fashion, O attack of the ketone enolate provides the product (Figure 2, bottom). Analogous calculations for the attack of the enolates derived from the model ester (methyl acetate) and nitro compound (nitromethane) point to the same conclusion. Therefore, it appears that transmetallation does not account for the observed differences in reactivity between these systems.

The immediate products of the transmetallation have a cyclic structure as they incorporate a weakly bound NaBr but converge after loss of the NaBr to η^3-bound enolates. For example, attack by the carbon center produces intermediates **prod 1k** and **prod 2 k** (see Figures 2 and 3), the form of which is higher in energy due to weaker binding of the enolate to the metal center.

Correspondingly, attack with the oxygen center of the enolate results in the formation of nearly degenerate structures **prod 3k** and **prod 4k**. The binding in these adducts is different from that observed in **prod 1k** and **prod 2k**. With the lone pair of oxygen involved in coordination, these intermediates maintain their initial η^3-binding to the Na atom while simultaneously binding to the Pd.

Upon decoordination of the NaBr, all four transmetallation products furnish isomeric η^3 complexes, **3_1** and **3_2** (Figure 3), both of which are slightly more stable than the oxidative addition adducts **iso1** and **iso2**, indicating that transmetallation is overall favorable. The stability of these adducts is likely defined by the efficiency of the orbital overlap. The larger, carbon-centered lobe of the enolate HOMO (highest occupied molecular orbital) undergoes a better overlap when interacting with the larger LUMO (lowest unoccupied molecular orbital) lobe, located trans to the ligand (Figure

https://dx.doi.org/10.1021/acs.joc.9b03203
J. Org. Chem. 2020, 85, 3465−3472

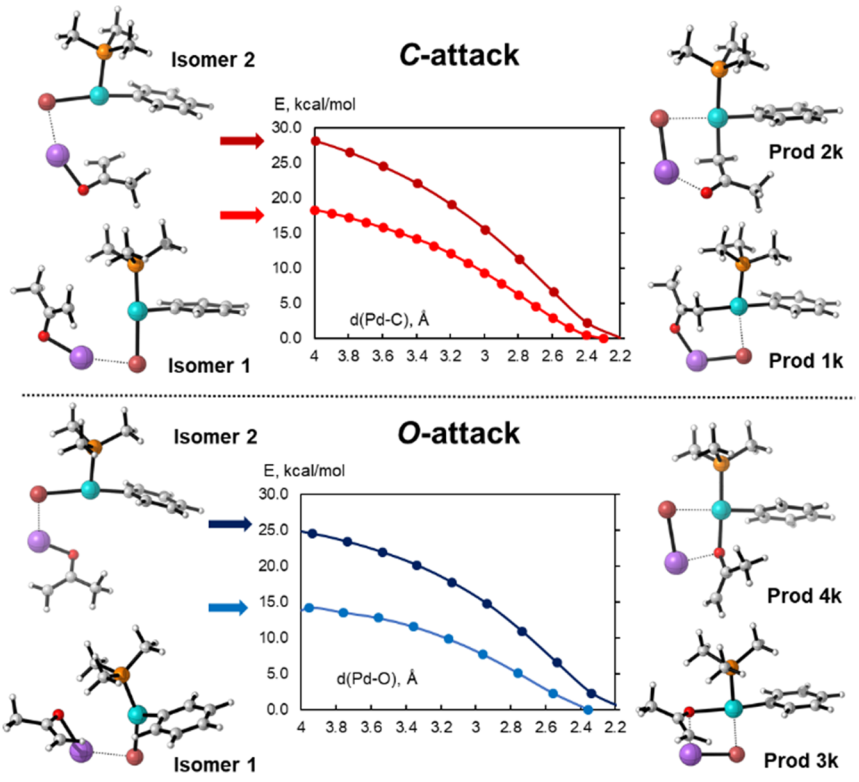

Figure 2. Energetics of C (red) and O (blue) attacks of the ketone sodium enolate on the isomers of $PMe_3PdPhBr$. Curves corresponding to the reaction of **iso1** are pictured in light color, while those representing reactivity of the **iso2** are dark. Values computed using relaxed PES scans along Pd-C and Pd-O bonds at rB3LYP/6-31G(d), Pd, Br: LANL2DZ theory level.

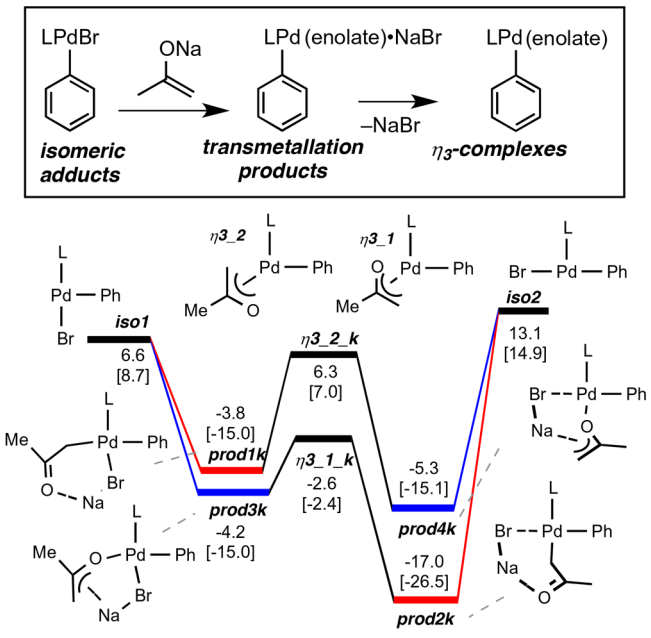

Figure 3. Transmetallation adducts and isomeric η^3–Pd complexes resulting from the carbon (red) or oxygen (blue) attacks by the ketone enolate on the isomers of $P(t\text{-}Bu)_3PdPhBr$. Labels for transmetallation products and η^3–Pd complexes are supplied with indices k, e, and n where k stands for ketone, e for ester, and n for nitro compound cases. Free energies and enthalpies (in brackets) are in kcal/mol.

4). As such, the ***η*3_1_k** complex is considerably more stable than the ***η*3_2_k** complex. Notably, this trend holds for all three of the enolates considered (see below). Coordination to the position trans to the phosphine is stronger for complexes **prod 1k** and **prod 2k** regardless of whether a C or O atom is present at this site (see bond lengths in Figure 4).

The energy diagram for the reaction of the ester enolate has a similar profile (Figure 5). Notable differences relative to the ketone include lower relative stability of the products of the O attack, **prod 3e** and **prod 4e**, as well as the intermediate **3_2_e**. Overall, the **3_1_e** complex is much more stable than the oxidative addition adducts **iso1** and **iso2** (Figure 3 vs Figure 5). All told, the net transmetallation of the ester enolate is substantially more favorable than for the ketone enolate.

Unlike the previous two cases, the nitronate exhibits a different reactivity (Figure 6). The ability to involve a second oxygen atom into binding allows the existence of the additional η^3 complex (**3_3_n** in Figure 6). All of the η^3 adducts (**3_1_n**, **3_2_n**, and **3_3_n**), despite having structures almost identical to those for the ketone and ester cases, are higher in energy relative to the oxidative addition adducts **iso1** and **iso2**, indicating an unfavorable transmetallation and giving a hint to the lower reactivity of these systems.

These observed trends in relative stability of the different intermediates can be reconciled using the hard–soft acid–base theory. The transmetallation step formally results in the exchange of the counterion for the corresponding enolate: The Na atom is replaced by the LPdAr fragment. The relative stability of the discussed adducts would be a direct consequence of the thermodynamics of such an exchange process. To provide a measure for this process, we evaluated the global and local softness of the corresponding enolates (Figure 7).

Using these softness parameters, we can explain the relative stability of the η^3 complexes. Perhaps unsurprisingly, the

https://dx.doi.org/10.1021/acs.joc.9b03203
J. Org. Chem. 2020, 85, 3465–3472

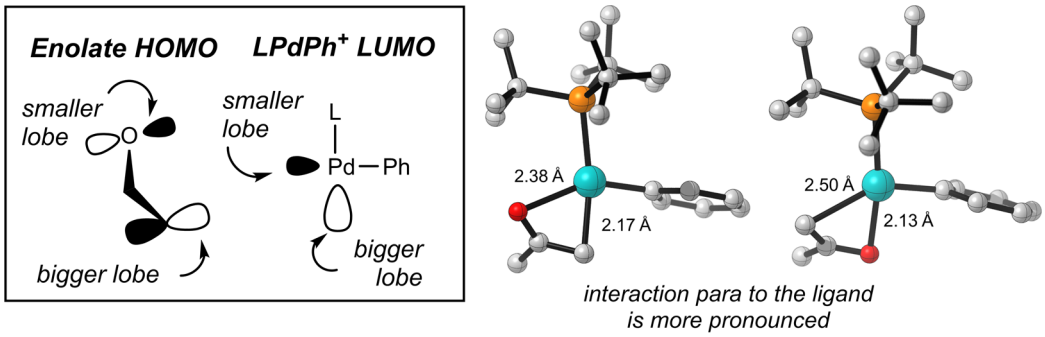

Figure 4. Left: HOMO of the enolate fragment and LUMO of the $LPdPh^+$. Right: structures of the η^3–Pd complexes resulting from a reaction with the ketone enolate.

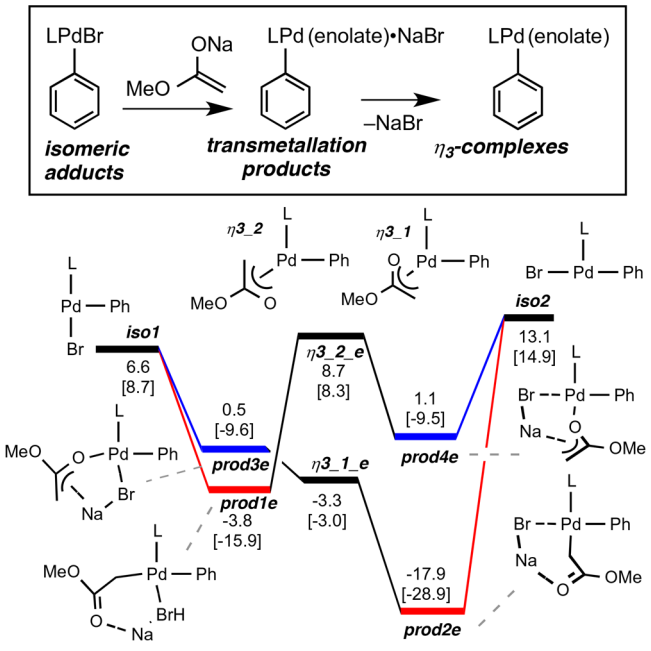

Figure 5. Transmetallation adducts and isomeric η^3–Pd complexes resulting from the carbon (red) or oxygen (blue) attacks by the ester enolate on the isomers of $P(t\text{-Bu})_3PdPhBr$. Free energies and enthalpies (in brackets) are in kcal/mol.

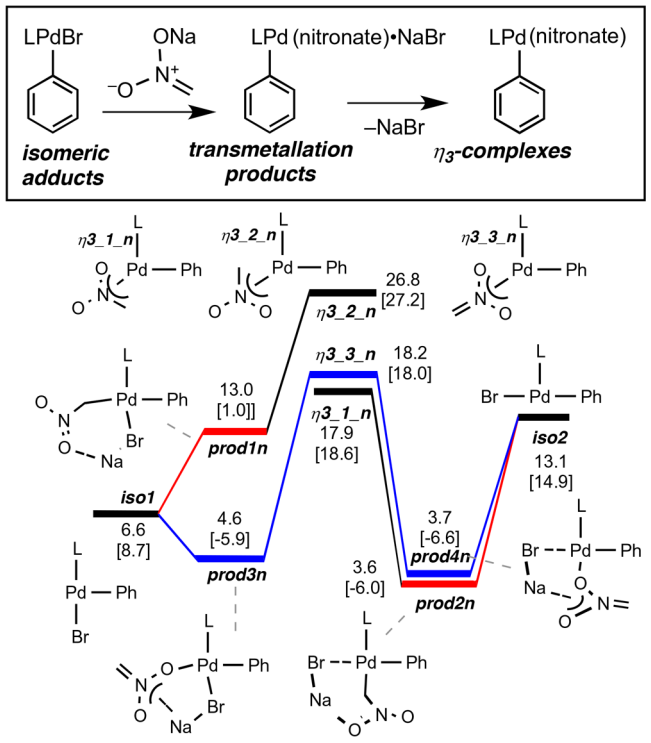

Figure 6. Transmetallation adducts and isomeric η^3–Pd complexes resulting from the carbon (red) or oxygen (blue) attacks by the nitronate on the isomers of $P(t\text{-Bu})_3PdPhBr$. Free energies and enthalpies (in brackets) are in kcal/mol.

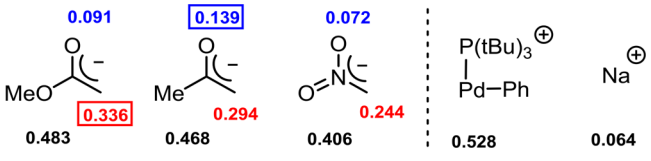

Figure 7. Global (in black) and local (blue for oxygen and red for carbon) softness parameters, eV^{-1}. Values computed using rB3LYP/6-311+G(d,p), Pd, Br: LANL2DZ, IEFPCM: toluene. Global softness was calculated as an inverse of hardness:[9] $S = 1/\eta$. In turn, global hardness was calculated from MO data using finite differences approximation:[10] $\eta \approx (I - A)/2$. Local softness was obtained from the global parameter using the nucleophilic Fukui function as approximated by HOMO density:[11] $s = Sf_- \approx S\rho_{HOMO}$

nitronate anion was found to be the hardest of the three as per both local and global parameters, indicating that an exchange of the hard counterion[12] (Na^+) for a soft one ($LPdPh^+$) would be the least favorable for this enolate. This analysis explains the significant relative destabilization of all the Pd–nitronate intermediates. Interestingly, the computed parameters indicate that the ester enolate has the softest carbon center while the ketone enolate has the softest oxygen. This result provides reasoning for the observed stability of the intermediates (Figure 8): Those that are controlled by the energy of the Pd–C bond would be the most stable for the enolate with the softest carbon (ester), while Pd–O intermediates are more stable for the enolate with the softest oxygen (ketone).[13]

In sum, the calculations indicate that upon loss of NaBr after transmetallation, the monophosphine Pd(II) adducts favor η^3 coordination over κ^1 modes. Furthermore, the favorability of transmetallation differs substantially across the series and is driven by hard/soft interactions.

C–C Reductive Elimination. Reductive elimination of both the three-membered and five-membered transition states was examined. The five-membered transition states corresponding to the acetate systems described by Gary and Sanford[14] were found to be unfavorable. Closer examination of the geometries of the five-membered transition states involving

https://dx.doi.org/10.1021/acs.joc.9b03203
J. Org. Chem. 2020, 85, 3465–3472

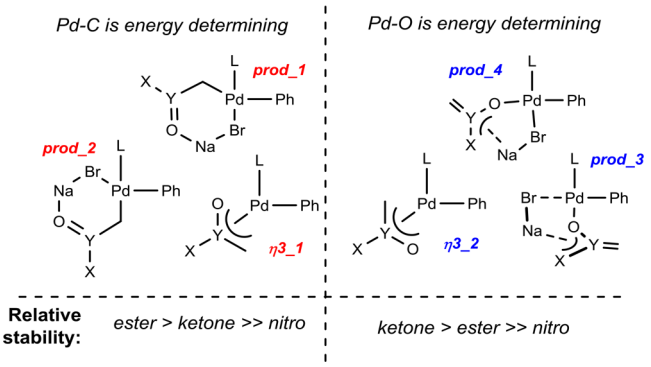

Figure 8. Relative stabilities of C-bound and O-bound enolates from ketones, esters, and nitroalkanes.

acetate suggests that electrons involved in the process are not a part of the allylic system, namely, the orthogonal lone pairs are utilized (Figure 9, left). In the case here, the enolate is only

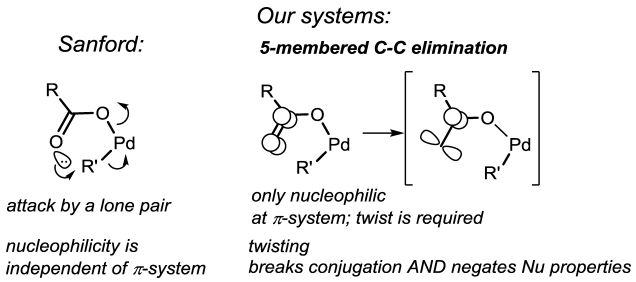

Figure 9. Orientation of orbitals for five-membered reductive elimination transition states.

nucleophilic via the π system. For nucleophilic attack to take place via a five-membered transition state, twisting of the π system is required, which is not favorable (Figure 9, right).

Calculations of the three types of coupling partners reveal that reductive elimination proceeds via the same type of three-membered transition states in all cases in accord with reported analyses of monoligated Pd complexes.[15] The preorganization of the different Pd–η^3 complexes described above dictates the outcomes of the reductive eliminations. Isomer **3_1** undergoes C–C reductive elimination, while only C–O elimination is possible for **3_2** (Figure 10.

For the nitro system, the energy of the corresponding reductive elimination transition states is much higher relative to those of the ketone and ester. This trend is in line with the relative local softness of the carbon centers in corresponding enolates. Based on this reactivity pattern, it appears that slow reductive elimination contributes to the low reactivity of nitro compounds under standard α-arylation conditions. Plotting the energy profiles on the same diagram highlights the difference between the three systems (Figure 11). Depending on the exact identity of the nitro species, reductive elimination can be a rate-limiting step altering the reactivity pattern to the extreme.

We further analyzed the reactivity of nitronates in α-arylation by computing key parts of the pathway for the reactions catalyzed by Buchwald ligands XPhos and *t*-Bu-XPhos (see Scheme 1 above). Together with P(*t*-Bu)$_3$, the performance of these two ligands in nitronate α-arylation has been studied experimentally in our laboratory.[5a] Notably, the identity of the ligand had a profound influence on the outcome

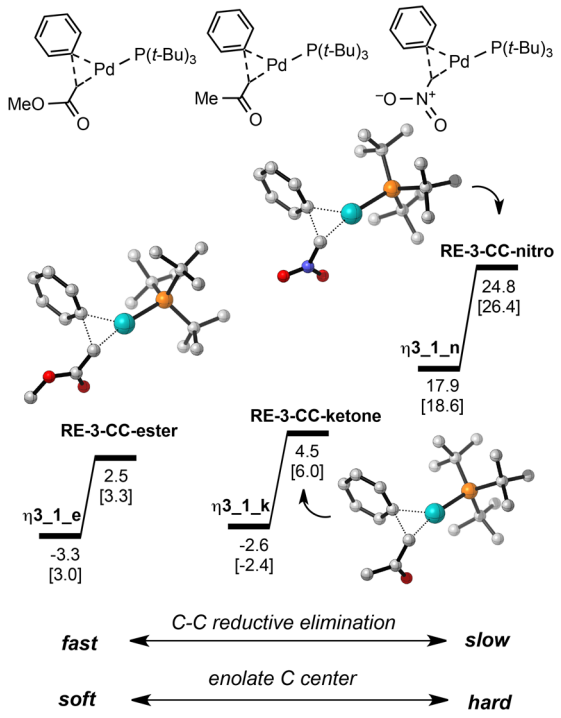

Figure 10. Energy profiles for C–C reductive elimination transition states. L = P(*t*-Bu)$_3$. Free energies and enthalpies (in brackets) are in kcal/mol.

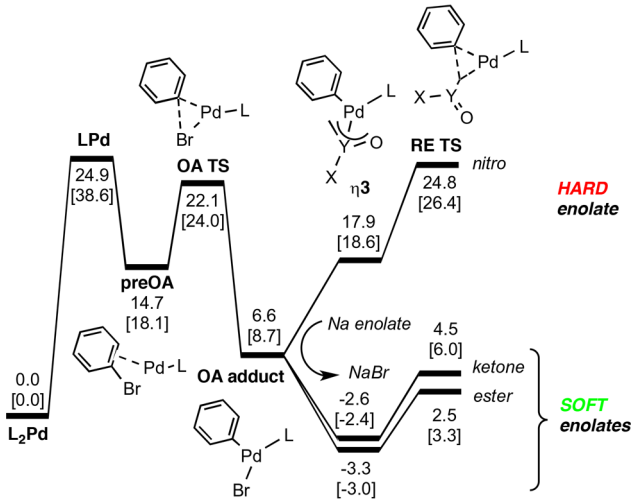

Figure 11. Overall energy profiles for the α-arylation of model ketone, ester, and nitro compound. Free energies and enthalpies (in brackets) are in kcal/mol.

with the XPhos ligand being the optimal for α-arylation of nitromethane. In contrast to trends seen for many other transformations, moving from this bis-cyclohexyl ligand to *t*-Bu-XPhos in this case resulted in significant drop in the efficiency of transformation.

Comparison of the computed *t*-Bu-XPhos and P(*t*-Bu)$_3$ profiles (Figure 12) reveals that both are very similar: Reductive elimination is the rate-limiting step while the oxidative addition is slightly lower in energy. The main difference between the two ligands is the nature of the starting Pd species. Extreme steric repulsion between *t*-Bu-XPhos ligands prevents the formation of L$_2$Pd species, resulting in LPd being the only available form of Pd^0. For the P(*t*-Bu)$_3$, the

https://dx.doi.org/10.1021/acs.joc.9b03203
J. Org. Chem. 2020, 85, 3465–3472

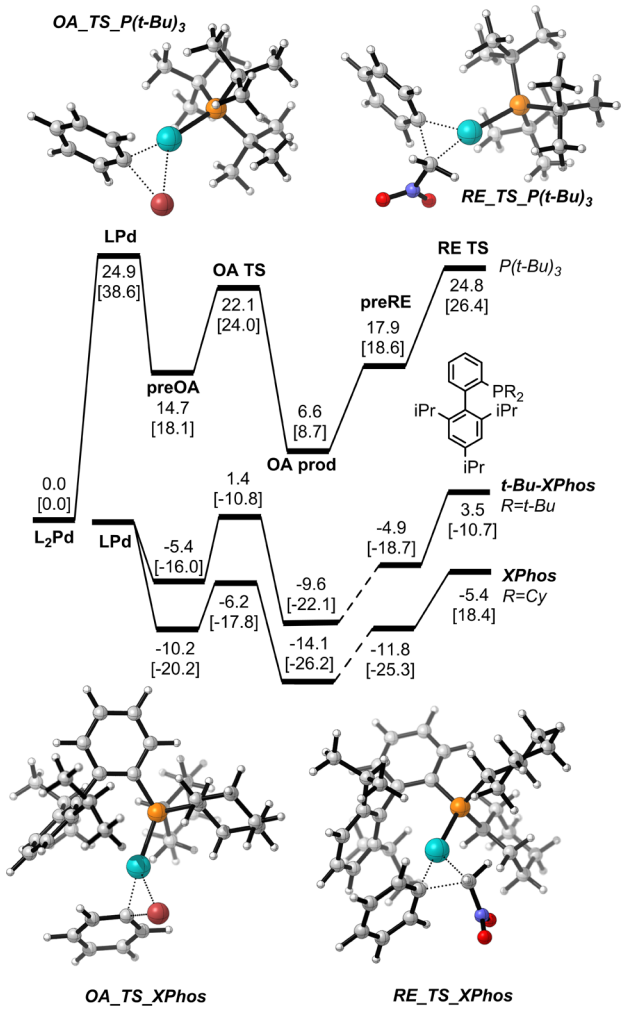

Figure 12. Energy profiles for the α-arylation of nitromethane using $P(tBu)_3$, XPhos, and *t*-Bu-XPhos ligands. In calculations, we used model ligands where the *para*-isopropyl group on the bottom ring is permuted to hydrogen. Free energies and enthalpies (in brackets) are in kcal/mol.

formation of L_2Pd is favorable. The different starting point for *t*-Bu-XPhos positions the entire reaction profile significantly lower on the energy diagram, making the corresponding transitions states much more accessible. Therefore, destabilization of bisligated Pd species is one of the main acceleration mechanisms contributing to high reactivity of Buchwald ligands. This finding is not enolate-specific and implies high reactivity of these ligands with both ketones and esters, which is indeed the case.[16]

In line with experimental observations, our calculations indicate a higher activity of the Pd-XPhos catalyst versus the Pd-*t*-BuXPhos catalyst (Figure 12). The reaction profiles between the two are very similar, with the main difference originating in the energy of association of the LPd with the starting PhBr. For XPhos, the association process is more exothermic, presumably due to lesser distortion of the sterically smaller XPhos upon binding of the LPd complex to PhBr. The distortion value is ~4 kcal/mol higher for *t*-BuXPhos, accounting for nearly all the difference in the energetics of association (see the Supporting Information for distortion interaction analysis). As the structures of the adducts are virtually identical (see Figure 13), the starting ligand geometry plays a key role. Specifically, the geometry of XPhos in the starting PdL is closer to that found in the coordination complex.

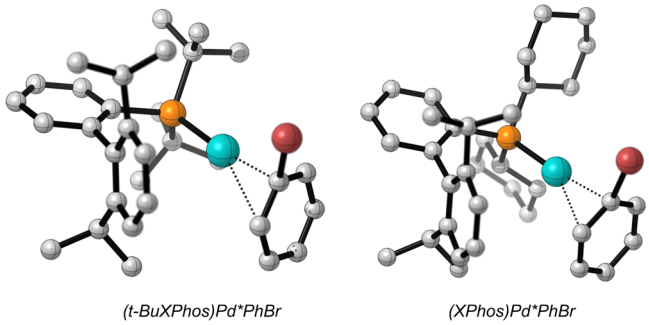

Figure 13. Geometries of coordination complexes of PdL with PhBr (preoxidation intermediates).

Another significant difference between the two ligands is the energy of reductive elimination. Even when the energy of association with PhBr is taken into account, the reductive elimination is still considerably faster for XPhos. This ligand is less electron-rich than *t*-Bu-XPhos, which facilitates reductive elimination.

C−O Reductive Elimination. Transmetallation can result in formation of the significantly less stable ***η*3_2** intermediates. Those are preorganized to undergo C−O reductive elimination. Interestingly, for all three systems, ***η*3_2** intermediates are less stable than corresponding C−C reductive elimination transition states. The high energy of the ***η*3_2** intermediates is significant and contributes to the difficulty observed for concerted C−O coupling.[17] As discussed earlier, destabilization of ***η*3_2** is likely a result of poor orbital overlap between the enolate and the LPdR fragment. This outcome can be improved by altering the electronics of the latter: Electron-poor ligands should stabilize ***η*3_2** intermediates, facilitating C−O coupling. This trend is indeed observed experimentally for C−O reductive eliminations.[18] This alteration, however, is likely to significantly affect other steps of the mechanism, thereby changing the energetics of the overall process. In particular, oxidative addition may become problematic.[19]

Analyzing C−O coupling, we found that eliminations via both three- and five-membered transition states are possible. Consistent with the findings reported by Sanford, five-membered transition states are more favorable (Figure 14). For the nitromethane system, however, the opposite is found (three-membered transition states are lower in energy), presumably due to the extremely low nucleophilicity of the nitronate oxygen. The general reactivity follows the same trend as that established for C−C couplings: enolates with softer centers (oxygen atom in this case) react faster. In all cases, C−O coupling is significantly higher in energy than the corresponding C−C coupling (c.f. Figure 10).

■ CONCLUDING REMARKS

To summarize, the reactivity of three enolate types in Pd-catalyzed arylations have been examined. The local softness of the enolate is instrumental in determining the relative energies of key intermediates and transition states. Soft centers provide the most favorable binding with Pd and stabilize the corresponding structures. The hardness of the nitronate anion dictates its low reactivity under standard arylation

https://dx.doi.org/10.1021/acs.joc.9b03203
J. Org. Chem. 2020, 85, 3465−3472

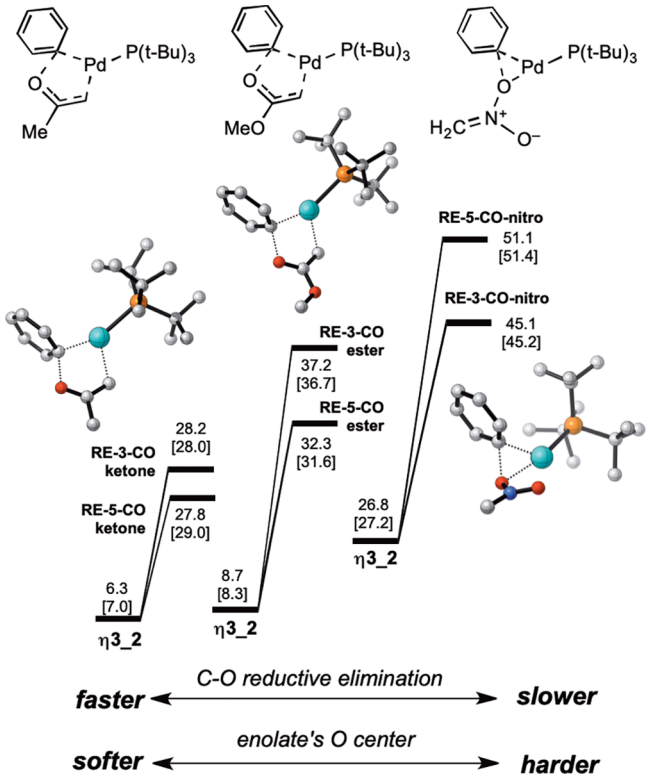

Figure 14. Energy profiles for C−O reductive elimination transition states. L = P(*t*-Bu)$_3$. Free energies and enthalpies (in brackets) are in kcal/mol.

conditions. Buchwald ligands accelerate the coupling of all enolate types by destabilizing the L_2Pd species. The higher activity of XPhos compared to *t*-BuXPhos in nitromethane arylation arises from less distortion of the XPhos ligand upon coordination of the aryl halide to the initial PdL complex. This lack of distortion combined with the less electron-rich character of XPhos contributes to its higher overall reactivity. It is expected that a detailed understanding of these systems and their trends will set the stage for rational ligand selection in related systems. For example, more substituted enolates will be softer which will offset the loss of reactivity from more hindered centers.

■ ASSOCIATED CONTENT

Supporting Information

The Supporting Information is available free of charge at https://pubs.acs.org/doi/10.1021/acs.joc.9b03203.

Computational methods, coordinates of located transition states and intermediates, and corresponding thermochemical data (PDF)

■ AUTHOR INFORMATION

Corresponding Author

Marisa C. Kozlowski − *Department of Chemistry, University of Pennsylvania, Philadelphia, Pennsylvania 19104, United States;* orcid.org/0000-0002-4225-7125; Email: marisa@sas.upenn.edu

Author

Sergei Tcyrulnikov − *Department of Chemistry, University of Pennsylvania, Philadelphia, Pennsylvania 19104, United States*

Complete contact information is available at: https://pubs.acs.org/10.1021/acs.joc.9b03203

Notes

The authors declare no competing financial interest.

■ ACKNOWLEDGMENTS

We are grateful to the NIH (R35 GM131902 and RO1 GM087605) and NSF (CHE1764298) for financial support of this research. We acknowledge XSEDE (TGCHEM120052) for computational resources.

■ REFERENCES

(1) (a) Bellina, F.; Renzo, R. Transition Metal-Catalyzed Direct Arylation of Substrates with Activated sp^3-Hybridized C-H Bonds and Some of Their Synthetic Equivalents with Aryl Halides and Pseudohalides. *Chem. Rev.* **2010**, *110*, 1082−1146. ((b)) Prim, D.; Marque, S.; Gaucher, A.; Campagne, J. (Ed). *Transition-Metal-Catalyzed α-Arylation of Enolates.* In Organic Reactions: 2012. (c) Johansson, C. C. C.; Colacot, T. J. *Angew. Chem. Int. Ed.* **2010**, *49*, 676−707. (d) Pilgrim, B. S.; Gatland, A. E.; Esteves, C. H. A.; McTernan, C. T.; Jones, G. R.; Tatton, M. R.; Procopiou, P. A.; Donohoe, T. J. Palladium-catalyzed enolate arylation as a key C−C bond-forming reaction for the synthesis of isoquinolines. *Org. Biomol. Chem.* **2016**, *14*, 1065−1090. (e) Gatland, A. E.; Pilgrim, B. S.; Procopiou, P. A.; Donohoe, T. J. Short and Efficient Syntheses of Protoberberine Alkaloids using Palladium-Catalyzed Enolate Arylation. *Angew. Chem. Int. Ed.* **2014**, *53*, 14555−14558.

(2) (a) Palucki, M.; Buchwald, S. L. Palladium-Catalyzed α-Arylation of Ketones. *J. Am. Chem. Soc.* **1997**, *119*, 11108−11109. (b) Moradi, W. A.; Buchwald, S. L. Palladium-Catalyzed α-Arylation of Esters. *J. Am. Chem. Soc.* **2001**, *123*, 7996−8002. (c) Hamann, B. C.; Hartwig, J. F. Palladium-Catalyzed Direct α-Arylation of Ketones. Rate Acceleration by Sterically Hindered Chelating Ligands and Reductive Elimination from a Transition Metal Enolate Complex. *J. Am. Chem. Soc.* **1997**, *119*, 12382−12383. (d) Kawatsura, M.; Hartwig, J. F. Simple, Highly Active Palladium Catalysts for Ketone and Malonate Arylation: Dissecting the Importance of Chelation and Steric Hindrance. *J. Am. Chem. Soc.* **1999**, *121*, 1473−1478. (e) Shaughnessy, K. H.; Hamann, B. C.; Hartwig, J. F. Palladium Catalyzed Inter- and Intramolecular α-Arylation of Amides. Application of Intramolecular Amide Arylation to the Synthesis of Oxindoles. *J. Org. Chem.* **1998**, *63*, 6546−6553. (f) Terao, Y.; Fukuoka, Y.; Satoh, T.; Miura, M.; Nomura, M. Palladium-catalyzed α-arylation of aldehydes with aryl bromides. *Tetrahedron Lett.* **2002**, *43*, 101−104. (g) Culkin, D. A.; Hartwig, J. F. Palladium-Catalyzed α-Arylation of Carbonyl Compounds and Nitriles. *Acc. Chem. Res.* **2003**, *36*, 234−245. and references cited therein (h) Jin, Y.; Chen, M.; Ge, S.; Hartwig, J. F. Palladium-Catalyzed, Enantioselective α-Arylation of α-Fluorooxindoles. *Org. Lett.* **2017**, *19*, 1390−1393. (i) Jiao, Z.; Beiger, J. J.; Jin, Y.; Ge, S.; Zhou, J. S.; Hartwig, J. F. Palladium-Catalyzed Enantioselective α-Arylation of α-Fluoroketones. *J. Am. Chem. Soc.* **2016**, *138*, 15980−15986.

(3) For typical procedures see ref 2g and references therein

(4) (a) Vogl, E. M.; Buchwald, S. L. Palladium-Catalyzed Monoarylation of Nitroalkanes. *J. Org. Chem.* **2002**, *67*, 106−111. (b) Muratake, H.; Nakai, H. Intramolecular cyclization using palladium-catalyzed arylation toward formyl and nitro groups. *Tetrahedron Lett.* **1999**, *40*, 2355−2358.

(5) (a) Walvoord, R. R.; Berritt, S.; Kozlowski, M. C. Palladium-Catalyzed Nitromethylation of Aryl Halides: An Orthogonal Formylation Equivalent. *Org. Lett.* **2012**, *14*, 4086−4089. (b) Metz, A. E.; Berritt, S.; Dreher, S. D.; Kozlowski, M. C. Efficient Palladium-Catalyzed Cross-Coupling of Highly Acidic Substrates, Nitroacetates. *Org. Lett.* **2012**, *14*, 760−763. (c) VanGelder, K. F.; Kozlowski, M. C. Palladium-Catalyzed α-Arylation of Aryl Nitromethanes. *Org. Lett.* **2015**, *17*, 5748−5751. (d) Walvoord, R. R.; Kozlowski, M. C. Minimizing the Amount of Nitromethane in Palladium-Catalyzed

Cross-Coupling with Aryl Halides. *J. Org. Chem.* **2013**, *78*, 8859−8864.
(6) Studies by Donald Watson on Ni and Cu-catalyzed alkylations of nitrocompounds are noteworthy (a) Rezazadeh, S.; Devannah, V.; Watson, D. A. Nickel-Catalyzed C-Alkylation of Nitroalkanes with Unactivated Alkyl Iodides. *J. Am. Chem. Soc.* **2017**, *139*, 8110−8113. (b) Gietter, A. A. S.; Gildner, P. G.; Cinderella, A. P.; Watson, D. A. General Route for Preparing β-Nitrocarbonyl Compounds Using Copper Thermal Redox Catalysis. *Org. Lett.* **2014**, *16*, 3166−3169. (c) Shimkin, K. W.; Gildner, P. G.; Watson, D. A. Copper-Catalyzed Alkylation of Nitroalkanes with α-Bromonitriles: Synthesis of β-Cyanonitroalkanes. *Org. Lett.* **2016**, *18*, 988−991.
(7) (a) Culkin, D. A.; Hartwig, J. F. C-C Bond-Forming Reductive Elimination of Ketones, Esters, and Amides from Isolated Arylpalladium(II) Enolates. *J. Am. Chem. Soc.* **2001**, *123*, 5816−5817. (b) Wolkowski, J. P.; Hartwig, J. F. Generation of Reactivity from Typically Stable Ligands: C−C Bond-Forming Reductive Elimination from Aryl palladium(II) Complexes of Malonate Anions. *Angew. Chem. Int. Ed.* **2002**, *41*, 4289−4291.
(8) (a) Fu, G. C. The Development of Versatile Methods for Palladium-Catalyzed Coupling Reactions of Aryl Electrophiles through the Use of $P(t\text{-}Bu)_3$ and PCy_3 as Ligands. *Acc. Chem. Res.* **2008**, *41*, 1555−1564. (b) Christmann, U.; Vilar, R. Monoligated Palladium Species as Catalysts in Cross-Coupling Reactions. *Angew. Chem. Int. Ed.* **2005**, *44*, 366−374. (c) Zapf, A.; Ehrentraut, A.; Beller, M. A New Highly Efficient Catalyst System for the Coupling of Nonactivated and Deactivated Aryl Chlorides with Arylboronic Acids. *Angew. Chem. Int. Ed.* **2000**, *39*, 4153−4155.
(9) (a) Yang, W.; Parr, R. G. Hardness, softness, and the Fukui function in the electronic theory of metals and catalysis. *PNAS* **1985**, *82*, 6723−6726. (b) Reed, J. L. Electronegativity: Chemical Hardness I. *J. Phys. Chem. A* **1997**, *101*, 7396−7400.
(10) (a) Pearson, R. G. Absolute electronegativity and absolute hardness of Lewis acids and bases. *J. Am. Chem. Soc.* **1985**, *107*, 6801. (b) Makov, G. Chemical Hardness in Density Functional Theory. *J. Phys. Chem.* **1995**, *99*, 9337.
(11) Berkowitz, M.; Parr, R. G. Molecular hardness and softness, local hardness and softness, hardness and softness kernels, and relations among these quantities. *J. Chem. Phys.* **1988**, *88*, 2554−2557.
(12) For experimental values for Na^+ see: Torrent-Sucarrat, M.; Geerlings, P. Analogies and differences between two ways to evaluate the global hardness. *J. Chem. Phys.* **2006**, *125*, 244101. and ref 4a
(13) Analysis of the stability of **prod 1** is more problematic due to the significant contribution of the steric interaction between enolate fragment and the ligand.
(14) Gary, J. B.; Sanford, M. S. Participation of Carbonyl Oxygen in Carbon−Carboxylate Bond-Forming Reductive Elimination from Palladium. *Organometallics* **2011**, *30*, 6143−6149.
(15) Tatsumi, K.; Hoffmann, R.; Yamamoto, A.; Stille, J. K. Reductive Elimination of d8-Organotransition metal Complexes. *Bull. Chem. Soc. Jpn.* **1981**, *54*, 1857−1867.
(16) Fox, J. M.; Huang, X.; Chieffi, A.; Buchwald, S. L. Highly Active and Selective Catalysts for the Formation of α-Aryl Ketones. *J. Am. Chem. Soc.* **2000**, *122*, 1360−1370.
(17) Concerted C-O reductive eliminations are rare and hard to promote. Stepwise mechanisms for these transformations are proposed: (a) Marquard, S. L.; Hartwig, J. F. *Angew. Chem. Int. Ed.* **2011**, *50*, 7119−7123. (a) Widenhoefer, R. A.; Buchwald, S. L. Electronic Dependence of C-O Reductive Elimination from Palladium (Aryl)neopentoxide Complexes. *J. Am. Chem. Soc.* **1998**, *120*, 6504−6511. Bespoke ligands are often required: (b) Vorogushin, A. V.; Huang, X.; Buchwald, S. L. Use of Tunable Ligands Allows for Intermolecular Pd-Catalyzed C−O Bond Formation. *J. Am. Chem. Soc.* **2005**, *127*, 8146−8149. and references cited therein (c) Zhang, H.; Ruiz-Castillo, P.; Buchwald, S. L. Palladium-Catalyzed C−O Cross-Coupling of Primary Alcohols. *Org. Lett.* **2018**, *20*, 1580−1583.
(18) Mann, G.; Shelby, Q.; Roy, A. H.; Hartwig, J. F. Electronic and Steric Effects on the Reductive Elimination of Diaryl Ethers from Palladium (II). *Organometallics* **2003**, *22*, 2775−2789.
(19) Hartwig, J. F. Electronic Effects on Reductive Elimination to Form Carbon−Carbon and Carbon−Heteroatom Bonds from Palladium (II) Complexes. *Inorg. Chem.* **2007**, *46*, 1936−1947.

https://dx.doi.org/10.1021/acs.joc.9b03203
J. Org. Chem. 2020, 85, 3465−3472